

Numerical Simulations of 15-Degree Inclined Dense Jets in Stagnate Water Over a Sloped Bottom



Xinyun Wang and Abdolmajid Mohammadian

1 Introduction

Inclined dense jets, or negatively buoyant jets are often discharged from desalination plants or wastewater treatment industrial outfall systems. This is required to obtain proper discharge specifications to make sure the brine has adequate mixing to minimize the risk to the marine creatures.

A sketch of inclined dense jet in stagnant water is shown in Fig. 1. The jet is discharged from the a round diffuser with initial velocity. It will reach the highest height and then falls back to the bottom and is then developed as a density current.

The experimental study on inclined dense jets has started and improved in the past 50 years. Zeitoun and McIlhenny [1] firstly carried out a laboratory experimental study with various inclinations. Roberts et al. [2] presented an experimental study of 60° jet inclination with PIV and LIF technology and defined parameters related to the jet mixing and developments. Lane-Serff et al. [3] conducted an experimental study on the dense jets with a wide range from 15° to 75°, the instability on the inner side of the jet was observed in their study. Shao and Law carried out an experimental study with inclination of 30 and 45 with LIF and PIV technology [4], they found the elevation of the discharge nozzle height, where the Coanda effect will influence the jet mixing, hence the boundary influence can not be ignored. Besides these, more and more experimental studies were carried out [5–9]. These experimental studies provided useful information of the inclined dense jet both in terms of geometrical and dilution information.

With the development of CFD (computational fluid dynamics), the numerical modeling has started to play an important role on prediction of the outfall systems. Vafeiadou et al. [10] were the first researchers to perform the numerical study of the

X. Wang (✉) · A. Mohammadian
University of Ottawa, Ottawa, Canada
e-mail: xwang457@uottawa.ca

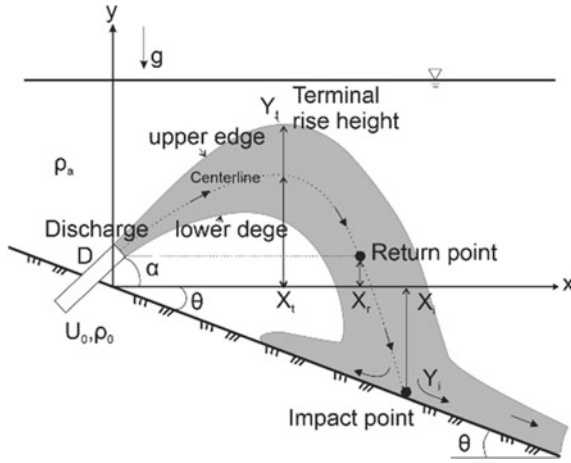


Fig. 1 Side view of inclined dense jet on a sloped bottom (slope angle θ) in stagnant water with inclination angle(α) (modified after [14])

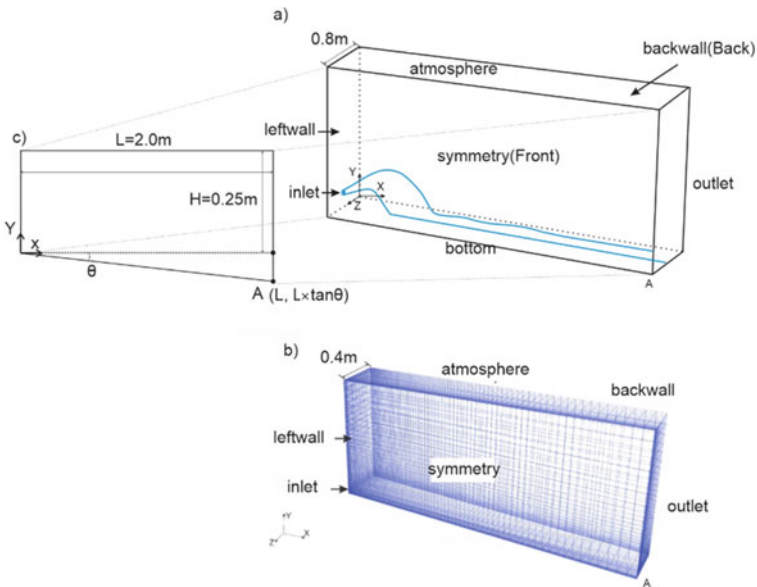


Fig. 2 **a** The experimental tank with sloped bottom; **b** Computational domain with mesh system; **c** x-y plane view

inclined dense jets. Their results had a good agreement with experimental studies. Oliver et al. [11] used the k-ε model for the simulation of the inclined dense jet. They initially calibrated the model with an experimental study on the vertical buoyant jets then applied it to the negatively buoyant jets. Kheirkhah Gildeh et al. [12] applied four different turbulence models to discover the performance of the models in prediction of the inclined dense jet with 45° and 60° in stagnant water. The Realizable k-ε and LRR turbulence model showed a better agreement with previous studies. Ardalan and Vafaei [13] also carried out a CFD study with the k-ε model with thermal-saline buoyant jets with a discharge angle of 45° in stationary water.

In many cases, the 60° discharge angle is considered as the design standard, however, with a shallow water depth, the jet will have a surface interaction which may cause a large area of brine pollution, so for a larger discharge angle, a larger water depth is needed. Considering that there is very limited research on the small discharge angle and with a sloped bottom, how the sloped bottom affects the development of the inclined dense jet with small inclination, is the main research topic in this study.

2 Methodology

2.1 Dimensional Analysis of Inclined Dense Jet

The side view of a typical inclined dense jet in stagnant water on a sloped bottom is shown in Fig. 1. The jet is discharged through a round nozzle of diameter (D) with velocity (U_0) and an initial angle α to the horizontal bottom (dash line), the sloped bottom with an inclination angle of θ , the ρ_0 and ρ_a are the density of the jet and receiving water respectively.

Return point and impact point can usually be treated as the same point in the horizontal situation. They should be addressed separately when there is a sloped bottom, or with a larger elevation.

All the flow properties can be represented related to three fluxes:

Flux of mass (Q_0), flux of momentum M and flux of buoyancy B_0 , which can be defined as $Q = \frac{\pi d^2 U_0}{4}$; $M = \frac{\pi d^2 H_0^2}{4}$; $B = g' Q$. From these fluxes, there are two important length scales that are commonly used in jet analysis: $L_m = \frac{M^{3/4}}{B^{1/2}}$ and $L_q = \frac{Q}{M^{1/2}}$

An important parameter related to jet study is densimetric Froude number, which can be presented as $Fr = \frac{U_0}{\sqrt{g_0 D}}$; $g'_0 = \frac{g(\rho_0 - \rho_a)}{\rho_a}$ or $L_m = \frac{M^{3/4}}{B^{1/2}} = (\frac{\pi}{4})^{1/4} D Fr$

All the geometrical properties such as jet highest location (X_t, Y_t), return point (X_r) and impact point X_i can be a function of Fr number and discharge angle. Similarly, this can be applied to the dilution properties [2], the dilution at y_i and return point or impact point S_m, S_r, S_i can be presented as $\frac{S_m}{Fr} = C1, \frac{S_r}{Fr} = C2, \frac{S_i}{Fr} = C3$. $C1, C2$ and $C3$ are the parameters which can be obtained from experimental studies.

2.2 Computational Setup

This study adopted the multi-fluid solver “twoLiquidMixingFoam” within the open source framework of OpenFoam to solve the Navier–stokes governing equations. A domain of 0.8 m width, 2 m length and 0.25 m height was considered for the numerical modeling setup. This flow problem is symmetric and a grid of 404,800 structured cells was found to be adequate in resolving the flow features for the given domain.

The nozzle diameter (D) for the inlet was 0.0108 m with 15° inclination. For the inlet, the boundary conditions were $U = 0.72 \frac{m}{s}$, $u = U \times \cos(\theta)$, $v = U \times \sin(\theta)$, $w = 0$, $k = 0.006u^2$, $\varepsilon = \frac{0.06u^3}{D}$, $T = 20^\circ\text{C}$. The surrounding water density was set to 998.2063 kg/m³. The initial conditions are listed in Table 1.

The flow was assumed to be incompressible in this study, the density for both jet and ambient water was calculated by Eq. (1) propose by Millero and Poisson [15]:

$$\rho = \rho_t + AS + BS^{2/3} + CS \quad (1)$$

where

$$A = 8.24493 \times 10^{-1} - 4.0899 \times 10^{-3}T + 7.6438 \times 10^{-5}T^2 - 8.2467 \times 10^{-7}T^3 + 5.3875 \times 10^{-9}T^4$$

$$B = -5.72466 \times 10^{-3} + 1.0227 \times 10^{-4}T - 1.6546 \times 10^{-6}T^2$$

$$C = 4.8314 \times 10^{-4}$$

ρ_t is the density of water, which varies with the temperature as follows:

$$\rho_t = 999.842594 + 6.793952 \times 10^{-2}T - 9.095290 \times 10^{-3}T^2 + 1.001685 \times 10^{-4}T^3 - 1.120083 \times 10^{-6}T^4 + 6.536336 \times 10^{-9}T^5 \quad (2)$$

Table 1 Initial conditions of the simulation

Diameter (m)	Velocity (m/s)	Froude number	Density deference (kg/m ³)	Jet density(kg/m ³)	L _m
0.0108	0.72	10	21.77179	1019.9781	0.101
0.0108	0.72	15	12.27659	1010.483	0152
0.0108	0.72	20	7.864012	1006.070	0.202
0.0108	0.72	25	5.45867	1003.665	0.253

3 Results and Discussion

3.1 Jet Trajectory and Flow Characteristics

The trajectory is the main geometrical characteristic of the jet. It can be derived from the maximum concentration or velocity contour map. Many studies stated that the concentration and velocity trajectory almost coincide with each other, [4, 16] while some studies argued that the concentration trajectory often descended faster than the velocity one [4, 12], this phenomenon can be found in this study (Fig. 3). For brevity, we only present the concentration trajectory. Figure 4 shows the trajectory of the jet on the horizontal bottom where the results have a good agreement with previous studies.

The trajectory of other sloped angle with different Froude number are also presented in Fig. 5. The dotted line presents the nominal horizontal bottom. The trajectory gets longer with a larger slope.

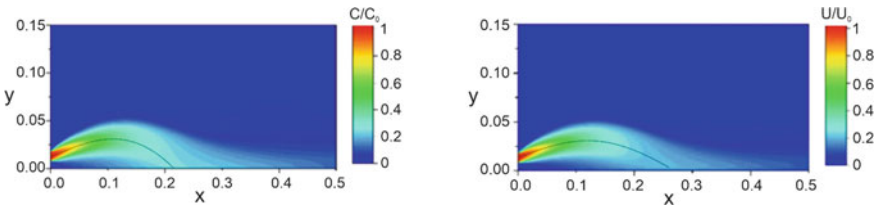
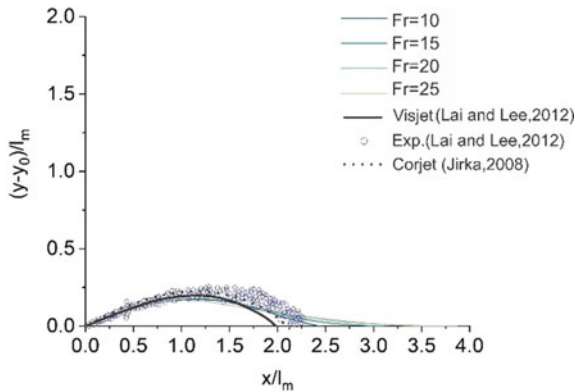


Fig. 3 a The concentration contour along the jet. b The velocity contour along the jet

Fig. 4 Normalized centerline trajectories ($\theta = 0^\circ$)



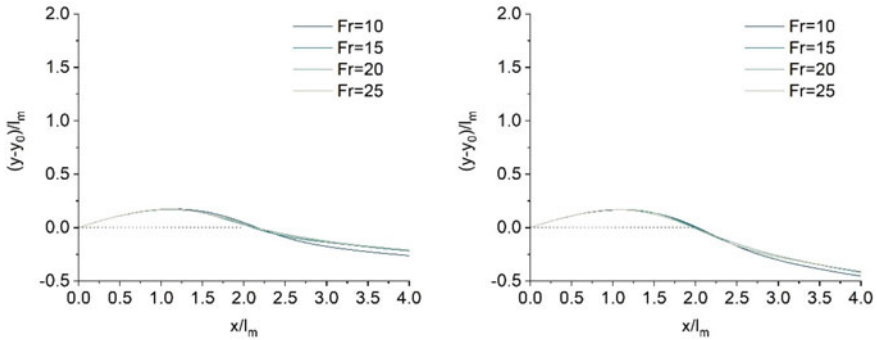


Fig. 5 Normalized centerline trajectories ($\theta = 3^\circ$ and $\theta = 6^\circ$)

3.2 Location of Terminal Rise Height

There are two methods to derive the terminal rise height, the first one obtains the 3% cut-off level of concentration from the jet centerplate [4] (Fig. 6a). Another method applies the 25% concentration contour of C_{max} (C_{max} = cross-section maximum concentration) [17] (Fig. 6b). In this study the first method based on $C = 3\%C_0$ is applied. The horizontal location of terminal rise height (X_t) can be easily obtained.

Kikkert et al. pointed out that the upper half of the jet is sharper than the lower part and it is closer to the jet centerline, which means the upper half of the jet is less affected by detrainment [18, 4]. Although this conclusion is carried out under the inclination of 30° , 45° or 60° , a similar trend can be found in this study (Fig. 7); the black contour line presents each 10% concentration difference. It is obvious that the lower half of the jet has more detrainment compared with the upper half.

The location where the jet touches the boundary is called return point or impact point or impingement point. Typically, the return point and impact point are not the same, because the return point is where the jet falls back to the same height as the discharge height, while, the impact point is where the jet touches the bed. When the discharge height is relatively small, these two points are treated as the same point.

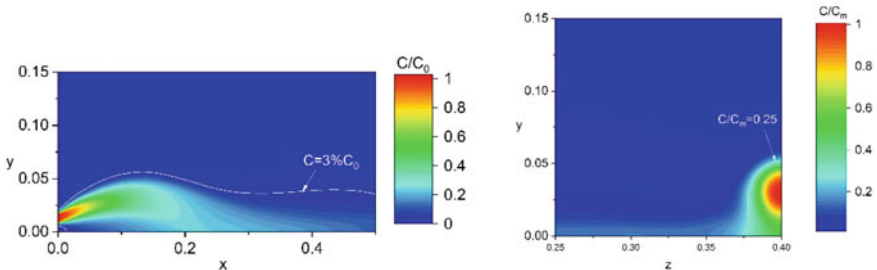
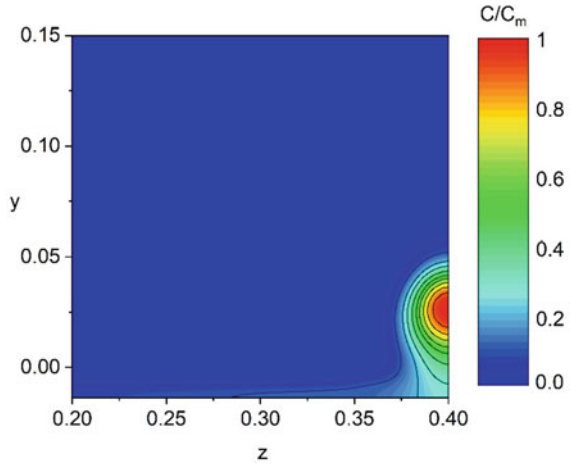


Fig. 6 Two methods for deriving the terminal rise height

Fig. 7 Concentration contour of vertical profile at the terminal rise height



Mixing is significantly reduced after the impingement takes place since the jet will move along the bottom with less detrainments. However, when the jet discharge height is higher or there is a slope at the bottom, these two points will show quite different properties.

3.3 The Location of the Return Point

The return point can be derived from the trajectory [4]. In this study, a slice (red line) at the same height as the discharge port are obtained (Fig. 8), the concentration is plotted against the horizontal location. The highest point represents the location of the return point and concentration. The horizontal location normalized by D and F is plotted in the Fig. 9. It shows that the jet will move further with a higher Fround number.

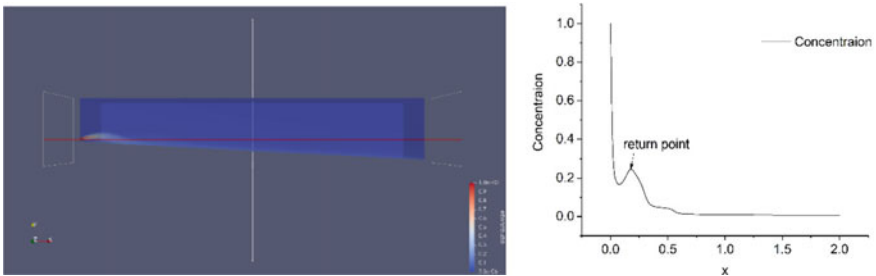


Fig. 8 Illustration of the method for return point

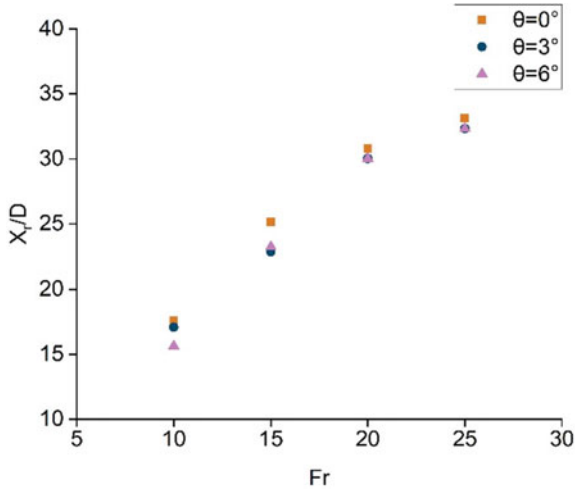


Fig. 9 Horizontal location of the return point (X_r) normalized by diameter (D) versus Froude number (Fr)

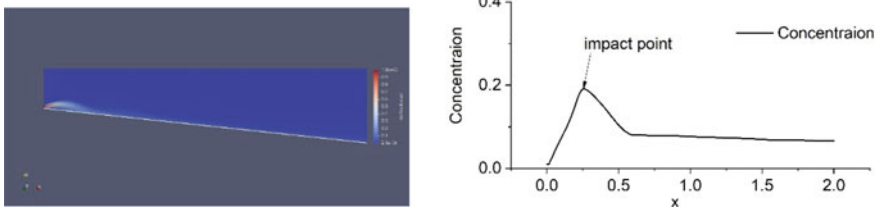


Fig. 10 Illustration of the method for finding the impact point

3.4 The Location of the Impact Point

The similar method of deriving the return point location is also applied here to find out the location of the impact point (Fig. 10).

The horizontal and vertical locations of the impact point are normalized with the L_m , as shown in Fig. 11. The jet moves further compared with the horizontal bottom.

3.5 Dilution at the Minimum Dilution Point, Return Point and Impact Point

The dilution at the terminal rise height, return point (impact point on a horizontal bottom) are also highly important in design applications. The impact point location and dilution are slope-related, so with different slope angles, the dilution is different.

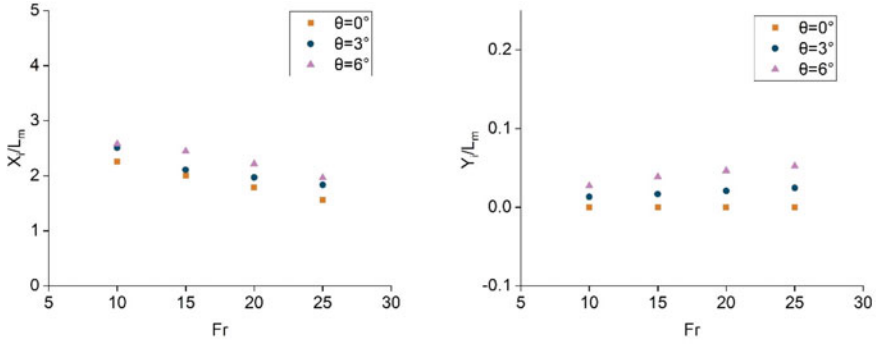


Fig. 11 Location of impact point for different Froude numbers and different slopes (Y_i is absolute value)

With a larger slope, the dilution at the impact point gets higher. All the geometric and dilution parameters are listed in Table 2.

3.6 The Dilution Variation on the Slope After the Impact Point

The jet eventually falls back to the bottom and as it moves along the bottom boundary, it will continue affecting the creatures growing on the sea bed.

Due to the limitation of the paper length, only $Fr = 10$ is presented here. Linear relations between the dilution (S/Fr) and horizontal location ($X/D Fr$) are shown in Fig. 12. Compared with the horizontal bottom, the mixing can be increased by 10% with a sloped bottom.

4 Conclusion

The results from a numerical investigation on the behaviour of the inclined dense jet over a sloped bottom by CFD have been presented. A discharge angle of 15° with 4 different initial conditions on three different slope angles (0° , 3° and 6°) are applied in OpenFOAM with a RANS turbulence model. This study aims to find out the jet development with a small discharge angle on a sloped bottom.

Geometrical and dilution properties were compared with the limited previous experimental data. The numerical and experimental results showed a good agreement and the slope affected the jet trajectory and dilution especially after the return point. The dilution on the slope showed a linear relation with the location on the slope. The jet not only moved downward, but it also spread out to both sides. The effect

Table 2 Geometric and dilution parameters from this study compared with previous studies

	Parameter	This study	Lai and Lee [19]	Visjet [19]	Kikkert [18]	Crowe [20]	Corjet [21]	Oliver [22]
Vertical location of terminal right height	Y_t/L_m	0.50	0.44	0.44	0.52	0.57	0.55	0.63
Horizontal location of terminal right height	X_t/L_m	1.30	1.22	1.19	1.47/1.22	1.45		1.4
Horizontal location of return point	X_r/L_m	1.64	2.41	2.15	2.53/2.13	2.51	1.9	2.39
Centerline Minimum dilution	S_m/ Fr	0.29	0.27	0.24		0.2(corjet) 0.23(visual plumes)		0.25
Return point dilution	S_r/ Fr	0.36	0.43	0.41			0.39	0.48
Impact point	S_i/ Fr	0.364($\theta = 0^\circ$) 0.421($\theta = 3^\circ$) 0.483($\theta = 6^\circ$)						

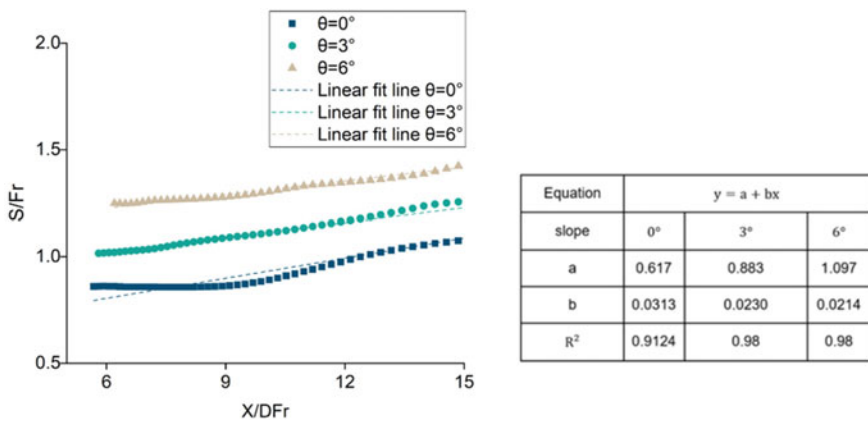


Fig. 12 Variation of jet dilution along the slope after the impact point ($Fr = 10$)

of boundary conditions on the inclined dense jet development will be addressed in a future study.

Acknowledgements The research was supported by Natural Sciences and Engineering Research Council of Canada (NSERC).

References

1. Zeitoun MA, McIlhenny WF (1971) Conceptual designs of outfall systems for desalination plants. In: Offshore technology conference
2. Roberts PJ, Ferrier A, Daviero G (1997) Mixing in inclined dense jets. *J Hydraul Eng* 123(8):693–699
3. Lane-Serff GF, Linden PF, Hillel M (1993) Forced, angled plumes. *J Hazard Mater* 33(1):75–99
4. Shao D, Law AWK (2010) Mixing and boundary interactions of 30° and 45° inclined dense jets. *Environ Fluid Mech* 10(5):521–553
5. Bashitialshaaer R, Larson M, Persson KM (2012) An experimental investigation on inclined negatively buoyant jets. *Water* 4(3):720–738
6. Bloomfield LJ, Kerr RC (2002) Inclined turbulent fountains. *J Fluid Mech* 451:283
7. Cipollina A, Brucato A, Grisafi F, Nicosia S (2005) Bench-scale investigation of inclined dense jets. *J Hydraul Eng* 131(11):1017–1022
8. Papakonstantis IG, Christodoulou GC, Papanicolaou PN (2011) Inclined negatively buoyant jets 1: geometrical characteristics. *J Hydraul Res* 49(1):3–12
9. Papakonstantis IG, Christodoulou GC, Papanicolaou PN (2011) Inclined negatively buoyant jets 2: concentration measurements. *J Hydraul Res* 49(1):13–22
10. Vafeiadou P, Papakonstantis I, Christodoulou G (2005) Numerical simulation of inclined negatively buoyant jets. In: The 9th international conference on environmental science and technology
11. Oliver CJ, Davidson MJ, Nokes RI (2008) $k-\epsilon$ Predictions of the initial mixing of desalination discharges. *Environ Fluid Mech* 8(5):617–625
12. Kheirkhah Gildeh H, Mohammadian A, Nistor I, Qiblawey H, Yan X (2016) CFD modeling and analysis of the behavior of 30° and 45° inclined dense jets—new numerical insights. *J Appl Water Eng Res* 4(2):112–127
13. Ardalan H, Vafaei F (2019) CFD and experimental study of 45° inclined thermal-saline reversible buoyant jets in stationary ambient. *Environ Process* 6:219–239
14. Jirka GH (2008) Improved discharge configurations for brine effluents from desalination plants. *J Hydraul Eng* 134(1):116–120. With permission from ASCE
15. Millero FJ, Poisson A (1981) International one-atmosphere equation of state of seawater. *Deep Sea Res Part A. Oceanogr Res Papers* 28(6):625–629
16. Zhang S, Jiang B, Law AWK, Zhao B (2016) Large eddy simulations of 45 inclined dense jets. *Environ Fluid Mech* 16(1):101–121
17. Jirka GH (2004) Integral model for turbulent buoyant jets in unbounded stratified flows. part i: single round jet. *Environ Fluid Mech* 4(1):1–56
18. Kikkert GA, Davidson MJ, Nokes RI (2007) Inclined negatively buoyant discharges. *J Hydraul Eng* 133(5):545–554
19. Lai CC, Lee JH (2012) Mixing of inclined dense jets in stationary ambient. *J Hydro-Environ Res* 6(1):9–28
20. Crowe A (2013) Inclined negatively buoyant jets and boundary interaction. Doctoral dissertation, University of Canterbury, Civil and Natural Resources Engineering

21. Bleninger T, Jirka GH (2008) Modelling and environmentally sound management of brine discharges from desalination plants. *Desalination* 221(1–3):585–597
22. Oliver CJ, Davidson MJ, Nokes RI (2013) Removing the boundary influence on negatively buoyant jets. *Environ Fluid Mech* 13(6):625–648